Digitoxin inhibits HeLa cell growth through the induction of G_2/M cell cycle arrest and apoptosis *in vitro* and *in vivo*

HUA GAN[1*], MING QI[2*], CHAKPIU CHAN[1*], PAN LEUNG[1], GENI YE[2], YUHE LEI[3], AIAI LIU[1], FEIFEI XUE[1], DONGDONG LIU[1], WENCAI YE[2], DONGMEI ZHANG[2], LIJUAN DENG[1] and JIAXU CHEN[1]

[1]Formula-pattern Research Center, School of Traditional Chinese Medicine, Jinan University; [2]Guangdong Province Key Laboratory of Pharmacodynamic Constituents of Traditional Chinese Medicine and New Drugs Research, Jinan University, Guangzhou, Guangdong 510632; [3]Department of Pharmacy, Shenzhen Hospital of Guangzhou University of Chinese Medicine, Shenzhen, Guangdong 518034, P.R. China

Received January 18, 2020; Accepted May 12, 2020

DOI: 10.3892/ijo.2020.5070

Abstract. Cervical cancer is the fourth most common gynecological malignancy affecting the health of women worldwide and the second most common cause of cancer-related mortality among women in developing regions. Thus, the development of effective chemotherapeutic drugs for the treatment of cervical cancer has become an important issue in the medical field. The application of natural products for the prevention and treatment of various diseases, particularly cancer, has always attracted widespread attention. In the present study, a library of natural products composed of 78 single compounds was screened and it was found that digitoxin exhibited the highest cytotoxicity against HeLa cervical cancer cells with an IC_{50} value of 28 nM at 48 h. Furthermore, digitoxin exhibited extensive antitumor activities in a variety of malignant cell lines, including the lung cancer cell line, A549, the hepatoma cell line, MHCC97H, and the colon cancer cell line, HCT116. Mechanistically, digitoxin caused DNA double-stranded breaks (DSBs), inhibited the cell cycle at the G_2/M phase via the ataxia telangiectasia mutated serine/threonine kinase (ATM)/ATM and Rad3-related serine/threonine kinase (ATR)-checkpoint kinase (CHK1)/checkpoint kinase 2 (CHK2)-Cdc25C pathway and ultimately triggered mitochondrial apoptosis, which was characterized by the disruption of Bax/Bcl-2, the release of cytochrome *c* and the sequential activation of caspases and poly(ADP-ribose) polymerase (PARP). In addition, the *in vivo* anticancer effect of digitoxin was confirmed in HeLa cell xenotransplantation models. On the whole, the findings of the present study demonstrate the efficacy of digitoxin against cervical cancer *in vivo* and elucidate its molecular mechanisms, including DSBs, cell cycle arrest and mitochondrial apoptosis. These results will contribute to the development of digitoxin as a chemotherapeutic agent in the treatment of cervical cancer.

Correspondence to: Dr Lijuan Deng or Professor Jiaxu Chen, Formula-pattern Research Center, School of Traditional Chinese Medicine, Jinan University, 601 West Huangpu Avenue, Guangzhou, Guangdong 510632, P.R. China
E-mail: ljdeng@jnu.edu.cn
E-mail: chenjiaxu@hotmail.com

*Contributed equally

Abbreviations: EMT, epithelial-mesenchymal transition; H&E, hematoxylin and eosin; IHC, immunohistochemistry; DSB, DNA double-stranded break

Key words: digitoxin, cervical cancer, G_2/M phase arrest, apoptosis

Introduction

Cervical cancer is the fourth most common gynecological malignancy affecting the health of women worldwide, with an estimated 570,000 new cases and 311,000 deaths in 2018. Moreover, the incidence of cervical cancer among young women is gradually increasing, and >85% of deaths related to cervical cancer occur in the developing world, rendering this type of cancer the second most common cause of cancer-related mortality in women living in developing regions (1,2). Although much progress has been made in the screening and prevention of cervical cancer, such as vaccination, some patients (approximately 6%) will inevitably be diagnosed with advanced, recurrent or metastatic cervical cancer. For these patients, chemotherapy, such as the combination of paclitaxel and cisplatin or paclitaxel, cisplatin and bevacizumab, remains a cornerstone of treatment (3-6). However, all these clinical chemotherapies for cervical cancer exhibit only limited effectiveness as tumor resistance eventually develops. Thus, the development of effective chemotherapeutic drugs for the treatment of cervical cancer has become an important issue in the medical field.

Natural products remain an important and promising source for the discovery of chemotherapeutic agents, such as the antimalarial drug, artemisinin. Camptothecin (derived from *Camptotheca acuminata*) and its clinical derivatives have been mainly applied for the clinical treatment of colon, lung, ovarian, breast, liver, pancreas and stomach cancers (7). Paclitaxel (isolated from *Taxus brevifolia*) and its derivatives have been approved for the management of metastatic breast cancer and metastatic breast cancer (8). Furthermore, from 1981 to 2014, approximately 49% of FDA-approved anticancer drugs were

derived either directly from natural resources or from their derivatives, including vinblastine and colchicine (9-14).

Digitoxin, a natural cardiac glycoside from *Digitalis*, has been used in the treatment of cardiac diseases for a number of years (15). Numerous experimental studies have demonstrated that digitoxin exhibits significant antitumor activities *in vitro* and *in vivo*, such as activities against renal cancer, breast cancer, melanoma (16), lung cancer (17,18), ovarian cancer (19,20), pancreatic cancer (21), glioma (22,23), prostate cancer (24), liver cancer (25) and colon cancer (26). It has been reported that the combination of digitoxin with anticancer agents leads to synergistic effects (27-29). Mechanistic studies have revealed that the promotion of apoptosis (21,22) and autophagy (20,30), the inhibition of angiogenesis (31), epithelial-mesenchymal transition (EMT) (24) and migration (19) and the suppression of cancer cell stemness (22,23) are involved in the anticancer effects of digitoxin. However, the anticancer effects and molecular mechanisms of digitoxin against HeLa cervical cancer cells have not yet been clearly defined.

In the present study, a library of natural compounds composed of 78 single compounds was screened to identify potential lead compounds with activity against cervical cancer. Several compounds were found to be of interest, and digitoxin was further evaluated in different malignant cell lines, including the cervical cancer cell line, HeLa, the lung cancer cell line, A549, the hepatoma cell line, MHCC97H, and the colon cancer cell line, HCT116. Mechanistically, it was found that digitoxin inhibited the proliferation of HeLa cells by blocking the cell cycle at the G_2/M phase via the ataxia telangiectasia mutated serine/threonine kinase (ATM)/ATM and Rad3-related serine/threonine kinase (ATR)-CHK1/checkpoint kinase 2 (CHK2)-Cdc25C pathway and triggering the activation of the mitochondrial apoptotic pathway. Furthermore, the *in vivo* anticancer effects of digitoxin were confirmed in HeLa cell xenotransplantation models. The findings of the present study provide support for the therapeutic potential of digitoxin in the treatment of cervical cancer.

Materials and methods

Chemical agents and antibodies. The library of natural compounds in listed in Table SI was obtained from Target Molecule Corp. The purities of these compounds were >95%, as determined by HPLC/UV analysis (data not shown). 3-(4,5-Dimethylthiazol-2-yl)-2,5-diphenyltetrazolium bromide (MTT) was purchased from Guangzhou Xueyou Biotechnology Co., Ltd. Propidium iodide (PI) and 4',6-dimidyl-2-phenylindole (DAPI) were purchased from Roche Diagnostics. The Annexin V-FITC/PI staining assay kit was obtained from Beyotime Institute of Biotechnology. The antibodies listed in Table SII were mainly purchased from Cell Signaling Technology and ProteinTech Group, Inc. The BCA protein assay kit and the enhanced chemiluminescent substrate were purchased from Jiangsu Keegan Biotechnology Co., Ltd.

Animals and cell lines. A total of 15 female BALB/c (nu/nu) nude mice (weighing 13-15 g, aged 4-5 weeks) were purchased from Vital River Laboratory Animal Technology Co., Ltd. and were used for the tumor xenograft experiments. Animals (5 animals/cage) were maintained at 22±2˚C coupled with 55±10% humidity under a 12 h light/dark cycle with free access to food and water. All animal experiments were conducted in compliance with the ARRIVE guidelines and were approved by the Experimental Animal Ethics Committee of Jinan University (Guangzhou, China).

The human cervical cancer cell line, HeLa, the liver cancer cell line, MHCC97H, the lung cancer cell line, A549 and the colorectal cancer cell line, HCT116, were obtained from the Chinese Academy of Sciences Cell Bank. All cells were cultured in Dulbecco's modified Eagle's medium (Gibco; Thermo Fisher Scientific, Inc.) with 10% fetal bovine serum (Gibco; Thermo Fisher Scientific, Inc.) and 1% (v/v) penicillin-streptomycin (Gibco; Thermo Fisher Scientific, Inc.) at 37˚C in an incubator with a humidified atmosphere and 5% CO_2. The HeLa cell line was identified by short tandem repeat (STR) profiling.

Measurement of cytotoxic activity. The cytotoxicity of the 78 natural products in the library against HeLa cells was screened by MTT assay. Cell suspensions were seeded in 96-well plates containing DMEM with 10% FBS and 1% (v/v) penicillin-streptomycin (PS) at a density of 5,000 cells per well. The plates were incubated at 37˚C (5% CO_2) for 24 h, and the medium was then replaced with fresh DMEM containing the test compounds (0.1 μM) for 72 h. The cells were then incubated with 0.5 mg/ml MTT solution for 3 h. The purple crystals were dissolved in dimethyl sulfoxide (DMSO), and the absorbance of each well was measured at 570 nm using a microplate reader (Epoch2, BioTek Instruments, Inc.).

Cell viability assay. HeLa, MHCC97H, A549 and HCT116 cells (5,000 cells/well) were plated in 96-well plates with various concentrations of the digitoxin ranging from 4 to 1,000 nM for 24 h and 48 h and then exposed to 0.5 mg/ml MTT for 3 h at 37˚C. The formazan crystals were dissolved in DMSO, and absorbance was measured at 570 nm on a microplate reader (Epoch2, BioTek Instruments, Inc.). The IC_{50} value was defined as the concentration of digitoxin with which the percentage inhibition was equal to 50 and was the mean from at least 3 independent experiments.

Cell cycle analysis. The cell cycle distribution of the HeLa cells was analyzed by PI staining assay. In brief, cells (200,000 cells/well) in 6-well plates were treated overnight with various concentrations of digitoxin (0, 4, 20, or 100 nM) for 24 h or with 20 nM digitoxin for 12, 24, or 36 h and then fixed with pre-cooled 75% ethanol at 4˚C for 24 h. Cells were incubated with PI (0.2 mg/ml) for 15 min at 37˚C in the dark. The PI fluorescence of the cells was analyzed using an EPICS-X flow cytometry (Beckman Coulter, Inc.), and the cell cycle distribution was analyzed using WINMDI v2.8 software (The Scripps Research Institute).

Apoptosis assay. A total of $5x10^5$ cells were seeded in 6-well plates and cultured overnight. The apoptotic rate of the cells was determined after 48 h of digitoxin treatment using the Annexin V-FITC/PI staining assay kit according to the manufacturer's instructions. Briefly, the cells were harvested and washed in PBS. The cells were then incubated with Annexin V for 15 min followed by PI for 5 min at 37˚C in the dark, final

analyzed in an EPICS-X flow cytometry (Beckman Coulter, Inc.), and cell apoptosis was analyzed using WINMDI v2.8 software (The Scripps Research Institute).

γH2AX staining. Immunofluorescence assays were performed as previously described (32). Briefly, cells (100,000 cells/dish) were incubated with digitoxin at 37˚C in a special culture dish used for confocal microscopy (20 mm) for 24 h and then fixed with 4% paraformaldehyde, permeabilized and blocked with QuickBlock™ Blocking Buffer (Beyotime). The cells were then incubated with γH2AX primary antibody (1:1,000) at 4˚C overnight. Subsequently, the cells were incubated for 2 h at room temperature and mounted. Images were observed under a microscope (Axio Vert. A1; Carl Zeiss AG).

Western blot analysis. Various concentrations of digitoxin (0, 4, or 20 nM) were added to the HeLa cells (2,000,000 cells/dish) in culture dishes (100 mm) for 24 h. Cellular proteins were then prepared, and extracts were prepared using lysis buffer (KeyGen) according to the manufacturer's instructions. The isolated cell lysate (40 μg) was separated by 10% SDS-PAGE and then transferred to PVDF membranes. The membranes were blocked with QuickBlock™ Blocking Buffer (Beyotime) and further immunoblotted with primary antibodies directed against ATM, ATR, CHK1, CHK2, Cdc25C, Bcl-2, cytochrome c, cleaved PARP, CDK1, Cyclin B1, Bax, caspase-3, caspase-9, cleaved caspase-3, cleaved caspase-9, and β-actin at a dilution of 1:1,000 overnight at 4˚C. A versatile imaging system for use with enhanced chemiluminescent substrates was used to visualize the protein bands. The membranes were then stripped with stripping buffer (Beyotime) and reblotted with phosphorylation site antibodies, including p-ATM (Ser1981), p-ATR (Ser428), p-Cdc25C (Thr48), p-CDK1 (Thr14), p-CHK2 (Thr68), p-CHK1 (Ser286) at a dilution of 1:1,000. The secondary antibody (1:5,000) consisting of peroxidase-conjugated goat anti-rabbit or anti-mouse IgG for 1 hour at room temperature. All the bands were visualized using enhanced chemiluminescence reagents (Millipore). ImageJ and GraphPad Prism v5.0 software were to measure the gray values and quantify the data of the bands.

Xenograft assay in nude mice. A sample of 5,000,000 HeLa cells was subcutaneously injected into the right flank of each mouse. When a tumor size of approximately 300 mm^3 was reached, the animals were randomly divided into 3 treatment groups (n=5). The vehicle group was intravenously administered 5% HS15 in saline. The digitoxin-treated groups were intraperitoneally administered digitoxin (dissolved in 5% HS15 in saline) at doses of 1 and 2 mg/kg. Tumor sizes were assessed every 2 days using calipers. Tumor volume was calculated using the following formula: $V = 0.5 \times a \times b^2$, where 'a' refers to the longer diameter and 'b' refers to the shorter diameter of the tumor. The treatment was terminated on day 19 as the size of one tumor was almost 2 cm in diameter. Animals were anesthetized with 1.5% isoflurane and then sacrificed by CO_2 inhalation. The flow rate of CO_2 in the euthanasia system displaced 30% of the cage volume/min. Tumors and hearts were collected, weighed and fixed in 4% paraformaldehyde. The tumor and heart tissues were further examined by hematoxylin and eosin (H&E) staining and immunohistochemistry (IHC).

Terminal deoxynucleotidyl transferase-mediated dUTP nick-end labeling (TUNEL) assay. Sections were permeabilized with proteinase K (Servicebio) working solution (20 μg/mL) for 25 min at 37˚C. After washing 3 times with PBS (pH 7.4) in a Rocker device (Servicebio), terminal deoxynucleotidyl transferase (TdT) and dUTP (Roche Diagnostics) were added to the sections followed by incubation at 37˚C for 2 h. The reaction was then stopped and followed by colorization with DAPI (Servicebio) for 10 min, kept in dark. Coverslips were subsequently mounted on glass slides with anti-fade mounting medium (Servicebio). Finally, the sections were analyzed under a light microscope (ECLIPSE C1, Nikon) and photographs of the sections were obtained. The number of TUNEL-positive cells were counted by an investigator who was blinded to the experimental design using Image-Pro Plus v6.0 software.

H&E staining and IHC. Tumor xenografts were fixed and then embedded in paraffin. Sections were cut at a thickness of 5 μm and mounted on glass slides. For histological examination, the sections were stained with H&E (Servicebio) 3 min at room temperature. To analyze apoptotic cells, the sections were examined using an *in situ* cell death detection kit (Roche Diagnostics) and antibodies against cleaved caspase-3 (1:1,000) over 24 h at 4˚C. To determine the proliferative index, the sections were incubated with a Ki-67 antibody (Cell Signaling Technology) (1:1,000) over 24 h at 4˚C. The stained sections in the present study were examined by a pathologist who was blinded to the treatment conditions. Images were acquired using an Olympus DP2-SAL microscope. Apoptosis (%) and the proliferative index (%) were analyzed using Image-Pro Plus v6.0 software.

Statistical analysis. Each experiment was performed at least 3 times, and the *in vitro* data are presented as the means ± SD and the *in vivo* data are presented as the means ± SEM. Statistical comparisons between groups were determined by one-way analysis of variance followed by a Tukey's post hoc test to determine the significant differences of means in multiple groups (n>2) comparisons using GraphPad Prism v5.0. $P<0.05$ was considered to indicate a statistically significant difference.

Results

Digitoxin is identified from the 78 natural products in the library screened against human cancer cells in vitro. The inhibitory effects of 78 natural compounds were tested in human cervical cancer HeLa cells by MTT assay. Based on the extensive literature published by researchers in combination with our own research experience, the concentration of 0.1 μM of the test compounds was selected (33-35). The results are expressed as cell growth inhibition and, as shown in Fig. 1A, the majority of the compounds exhibited no cytotoxicity towards HeLa cells; however, docetaxel trihydrate (no. 55), colchicine (no. 64), berberine hydrochloride (no. 32) and doxorubicin hydrochloride (no. 69) significantly inhibited the proliferation of HeLa cells, and the cell growth inhibition rate was 60-80% at a concentration of 0.1 μM. Importantly, digitoxin (no. 63; chemical structure shown in Fig. 1B) was identified as the most cytotoxic compound in HeLa cells.

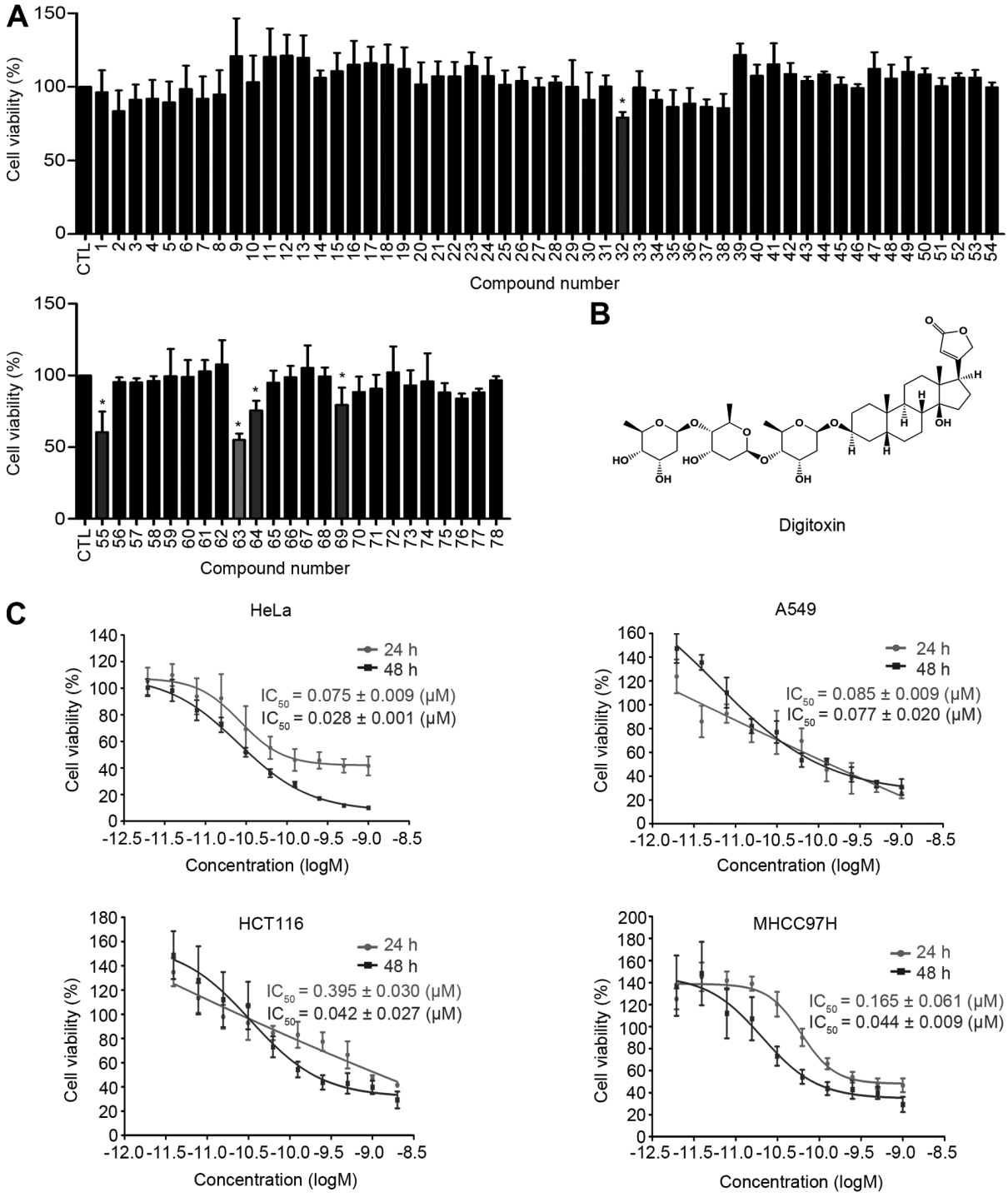

Figure 1. Identification of digitoxin from the 78 natural products in the library screened against human cancer cells in vitro. (A) *In vitro* cytotoxicity of digitoxin in HeLa cells. The inhibitory effects of 78 natural compounds (0.1 μM) on HeLa cells were determined by MTT assay following treatment with digitoxin. (B) Chemical structure of digitoxin. (C) Digitoxin inhibited the cell proliferation of 4 types of cancer cells in a dose- and time-dependent manner. Each column represents the mean ± SD (n=3). Data are shown as the means ± SD of 3 replicates. *P<0.01 vs. control.

Subsequently, the growth inhibition curves of digitoxin were further examined in several types of malignant cells, including MHCC97H, A549, HCT116 and HeLa cells. As shown in Fig. 1C, digitoxin potently decreased the viability of these cancer cells in a dose- and time-dependent manner, with the IC_{50} values ranging from 0.075 to 0.395 μM following digitoxin treatment for 24 h and from 0.028 to 0.077 μM following digitoxin treatment for 48 h. When comparing the IC_{50} values, the HeLa and A549 cells exhibited a greater sensitivity to digitoxin than the other cell lines, HCT116 and MHCC97H. These results indicate that digitoxin has a broad spectrum of antitumor effects *in vitro*. The HeLa cell line was selected for the investigation of the anticancer mechanism of digitoxin, since it has the highest sensitivity towards this natural compound.

Digitoxin disrupts the cell cycle. To investigate whether digitoxin disrupts the cell cycle, the DNA content of the digitoxin-treated cells was analyzed. The cell population

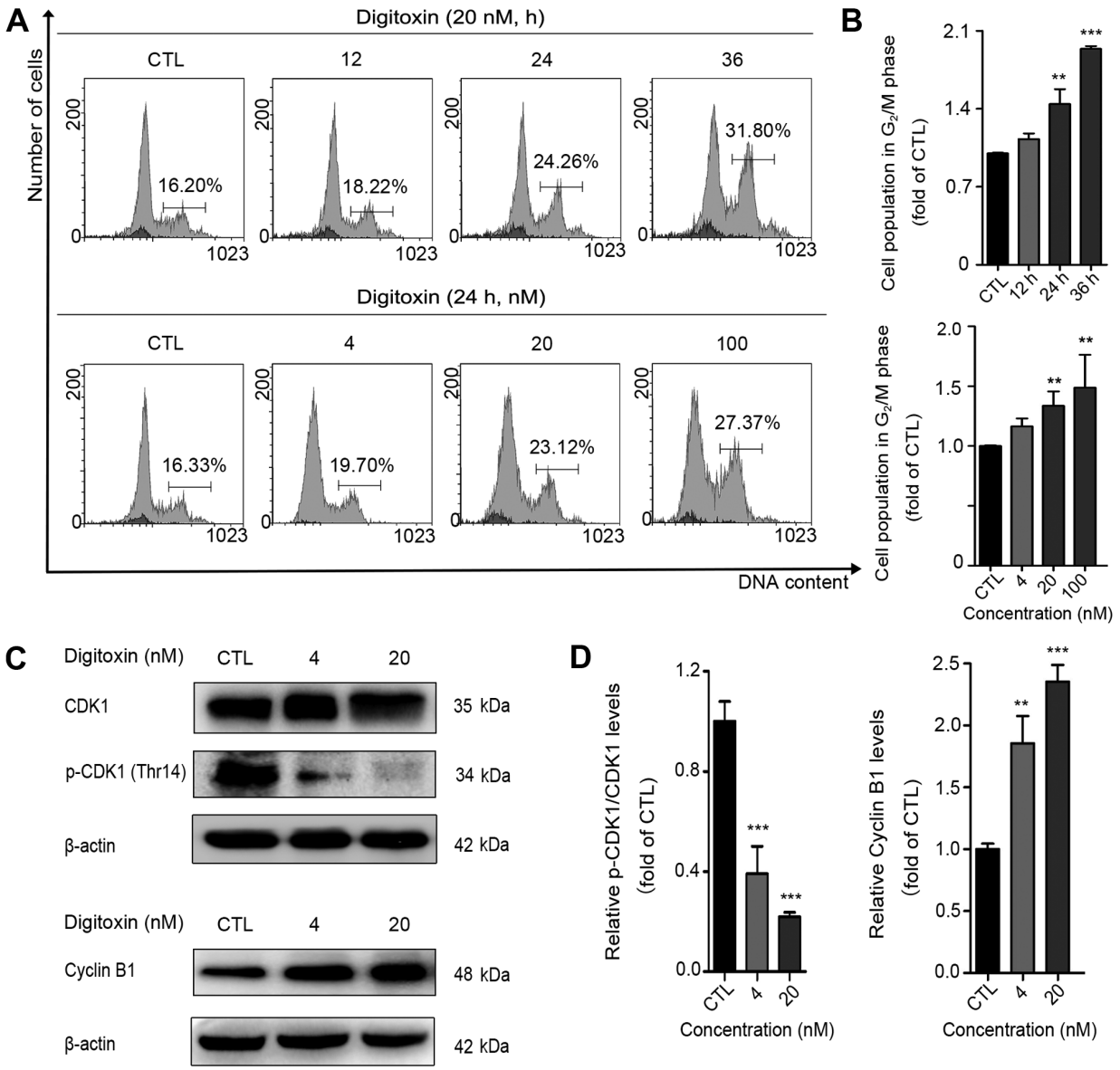

Figure 2. Digitoxin disrupts the cell cycle. (A) Digitoxin increased the cell population in the G_2/M phase. After treatment with or without digitoxin (20 nM) for 24, 36 and 48 h, the cell cycle distribution was measured by PI staining assay. Representative images are shown. (B) Quantification of the cell population in the G_2/M phase. Each column represents the mean ± SD (n=3). **P<0.01, ***P<0.001 vs. the control group. (C) Digitoxin inhibited CDK1 and Cyclin B1. HeLa cells were treated with or without digitoxin (4 and 20 nM) for 24 h, and the levels of CDK1, cyclin B1 and p-CDK1 (Thr14) were evaluated by western blot analysis. β-actin was used as the loading control. (D) Quantitative data of the relative protein expression are shown as the means ± SD (n=3). **P<0.01, ***P<0.001 vs. the control group.

in the G_2/M phase increased from 16.27 to 18.36, 23.46 and 31.51% in the presence of digitoxin (20 nM) for 12, 24 and 36 h, respectively (data presented in the text are the average of 3 experiments). Moreover, when the cells were exposed to digitoxin at concentrations of 4, 20 and 100 nM for 24 h, the cell population in the G_2/M phase markedly increased from 16.27 to 28.07% (data presented in the text are the average of 3 experiments; Fig. 2A and B). In animal cells, the G_2/M transition is regulated by the activity of CDK1, which is regulated by phosphorylation, and the concentration of cyclin B (36). In the present study, to further reveal the molecular mechanisms responsible for digitoxin-induced G_2/M arrest, the levels of these two key regulators, CDK1 and cyclin B1, were examined. As shown in Fig. 2C and D, digitoxin significantly decreased the protein expression levels of total CDK1 and phosphorylated CDK1 (p-CDK1 Thr14). Digitoxin treatment led to a marked accumulation of the cyclin B1 protein, further suggesting that HeLa cells treated with digitoxin are mainly blocked at the G_2/M phase.

Digitoxin induces G_2/M phase arrest via the activation of the ATM pathway. It is well known that DNA damage may be responsible for G_2/M cell cycle arrest (37). In the present study, to investigate whether the digitoxin-induced cell cycle arrest at the G_2/M phase was related to DNA lesions, an immunofluorescence staining assay was performed to measure the expression level of p-γH2AX, a marker of DNA double-stranded breaks (DSBs) (38). The results revealed the accumulation of γH2AX (Fig. 3A and B). ATM and ATR are activated by phosphorylation following DNA

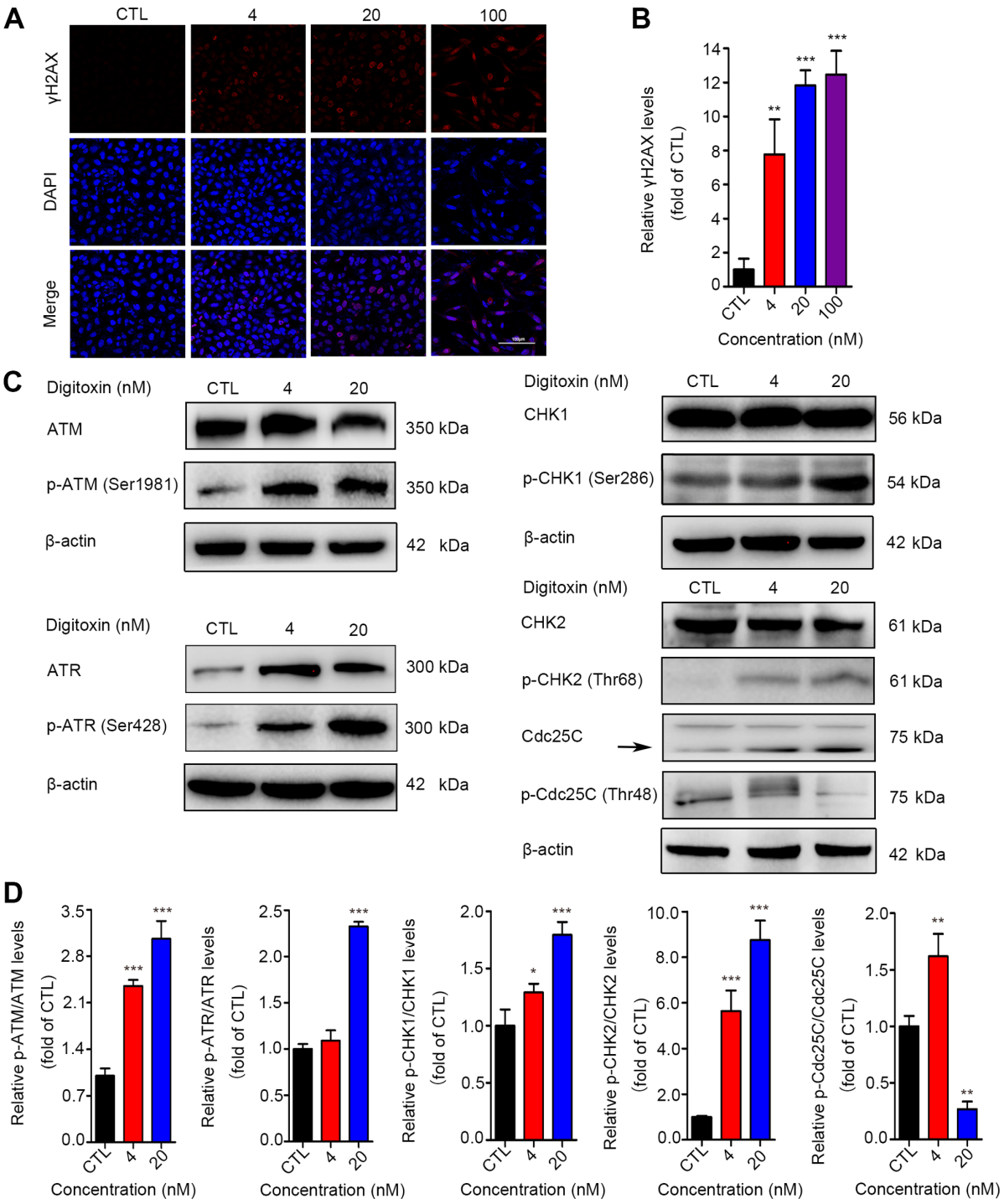

Figure 3. Digitoxin-induced G_2/M phase arrest via the ATM pathway. (A) Immunofluorescence of γH2AX. HeLa cells were treated with digitoxin (4, 20, or 100 nM) or not for 24 h. γH2AX-positive cells were identified by immunofluorescence staining. Images were obtained at x200 magnification (scale bar, 100 μm). (B) Quantitative data of the γH2AX fluorescence intensities. Data are expressed as the means ± SD (n=3). **P<0.01, ***P<0.001 vs. the control group. (C) Digitoxin activated the ATM signaling pathway. The expression levels of ATM, p-ATM (Ser1981), ATR, p-ATR (Ser428), CHK1, p-CHK1 (Ser286), CHK2, p-CHK2 (Thr68), Cdc25C and p-Cdc25C (Thr48) were examined by western blot analysis. β-actin served as the reference protein. (D) Quantitative data of the relative protein expression are illustrated as the means ± SD (n=3). *P<0.05, **P<0.01, ***P<0.001 vs. the control group.

damage, and phosphorylated ATM and ATR block the cell cycle partly through the activation of the checkpoint kinases CHK1 and CHK2. Active CHK1 and CHK2 then decrease Cdc25C activity, which prevents the dephosphorylation of CDK1 (Tyr15 and Thr14) to maintain the CDK1-Cyclin B1 complex in an inactive state (37,39-41). In the present study, as shown in Fig. 3C and D, the levels of p-ATM (Ser1981), p-ATR (Ser428), p-CHK1 (Ser286) and p-CHK2 (Thr68) were significantly upregulated in the digitoxin-treated cells. The level of phosphorylated Cdc25C was decreased in the digitoxin-treated HeLa cells. Collectively, these results demonstrated that digitoxin caused DNA damage to block the cell cycle at the G_2/M phase by triggering the activation of the ATM/ATR-CHK1/CHK2-Cdc25C signaling pathway.

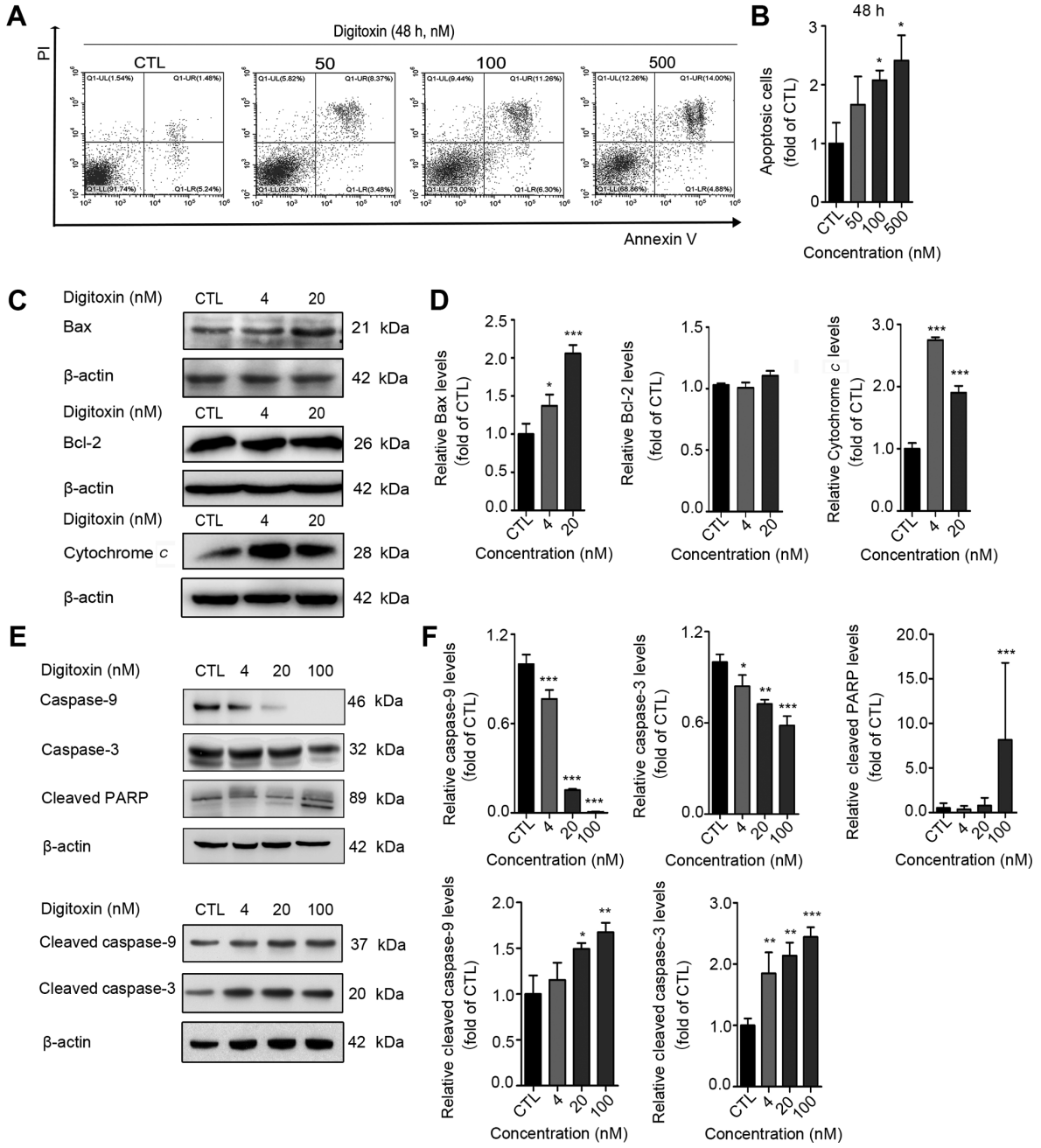

Figure 4. Digitoxin activates mitochondrial apoptosis. (A) Digitoxin induced apoptosis of HeLa cells. Cells were harvested and assayed by Annexin V-FITC/PI staining assay. Representative images show a concentration-dependent effect of digitoxin. (B) Quantitative data of digitoxin-induced apoptosis. Data are expressed as the means ± SD (n=3). *P<0.05 vs. the control group. (C) Digitoxin disrupted the interaction between Bax and Bcl-2 and released cytochrome c. The expression levels of Bax, Bcl-2 and cytochrome c were evaluated by western blot analysis. β-actin served as the reference protein. (D) Quantitative data of relative protein expression are shown as the means ± SD (n=3). *P<0.05, ***P<0.001 vs. the control group. (E) Digitoxin facilitates the activation of caspase-3, caspase-9 and PARP. The expression of caspase-9, caspase-3, cleaved caspase-9, cleaved caspase-3 and cleaved PARP was detected. β-actin was used as the loading control. (F) Quantitative data of the relative protein expression are shown as the means ± SD (n=3). *P<0.05, **P<0.01, ***P<0.001 vs. the control group.

Digitoxin activates mitochondrial apoptosis. To determine whether digitoxin induces cell apoptosis, an Annexin V-FITC/PI double staining assay was performed. HeLa cells were treated with increasing concentrations of digitoxin (20, 100 and 500 nM) for 48 h. The apoptotic ratio of HeLa cells increased by approximately 2-fold from 8.95 to 23.77% at 48 h (data in the text are the average of 3 experiments; Fig. 4A and B). To investigate whether digitoxin-induced apoptosis is mediated by the mitochondrial pathway, the changes in the levels of Bax/Bcl-2 were analyzed. As was expected, Bax expression was upregulated and Bcl-2 expression was almost unaltered in the digitoxin-treated cells (Fig. 4C and D). Moreover, it was found that the expression of cytochrome *c* was significantly increased in the digitoxin-treated cells (Fig. 4C and D). In addition, the caspase signaling pathway was activated, which was characterized by the downregulation of caspase-9 and caspase-3, and the upregulation of cleaved caspase-9, cleaved Caspase-3 and cleaved poly(ADP-ribose) polymerase (PARP) (Fig. 4E and F). Taken together, these results indicated that digitoxin triggered the activation of the mitochondrial apoptotic pathway in HeLa cells.

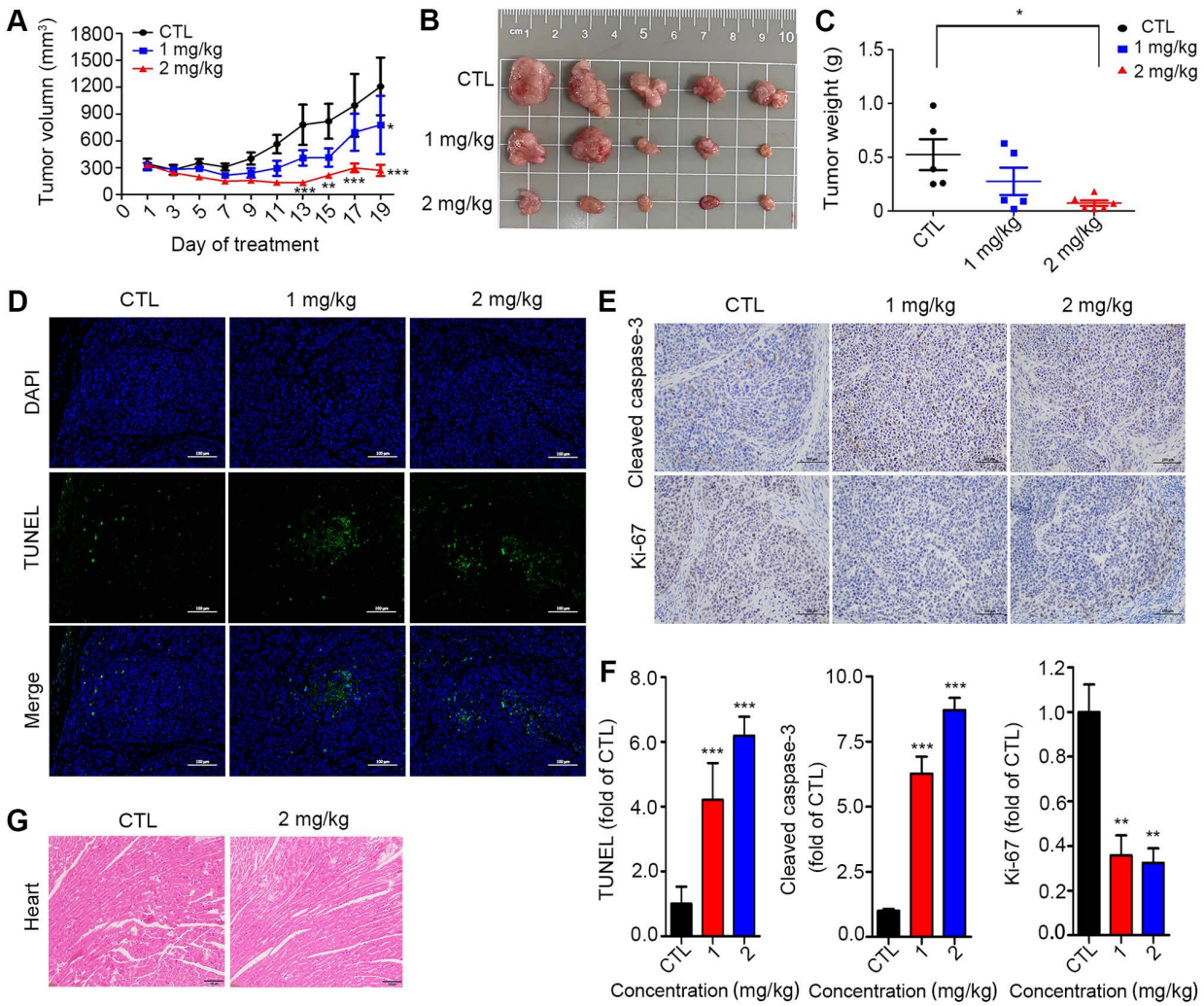

Figure 5. Anticancer effect of digitoxin in vivo. (A) Growth curves of subcutaneous xenografts of HeLa cells. Nude mice were randomized into 3 groups (n=5) and intraperitoneally injected with digitoxin (1 or 2 mg/kg) each day for a period of 19 days. Tumor volume was recorded every 2 days. The tumor volume (mm^3) of the HeLa xenografts is shown as the mean ± SEM. **P<0.01, ***P<0.001 vs. the group without digitoxin treatment [control (CTL)]. (B) Representative images of HeLa-derived tumor xenografts (n=5). (C) Tumor weight of HeLa xenografts (n=5). *P<0.05 vs. the group without digitoxin treatment. (D and E) Immunohistochemistry was conducted with a TUNEL staining kit, anti-cleaved caspase-3 and anti-Ki-67 antibodies. Representative images are shown. Images were obtained at magnification, x200 (scale bar, 100 μm). (F) Quantification of TUNEL (%), cleaved caspase-3 and Ki-67 staining was calculated using Image-Pro Plus v6.0 software. Each column represents the mean ± SEM (n=5). **P<0.01, ***P<0.001 vs. the 5% Solutol-HS15 control. (G) Representative images of morphological changes in the myocardium. Heart tissues were observed by H&E staining. Original magnification, x20; scale bar, 100 μm.

Anticancer effects of digitoxin in vivo. The antitumor effects of digitoxin were examined in nude mice harboring HeLa tumor xenografts. As shown in Fig. 5A and B, the tumor volume in the vehicle control group increased from 344.78±39.25 to 1054.18±414.04 mm^3, while the tumor volume in the digitoxin-treated group (2 mg/kg) increased from 330.71±45.61 to 214.56.93±73.25 mm^3, demonstrating that digitoxin treatment exerted a tumor-suppressive effect. The tumor weight of the digitoxin-treated group was much lower than that of the control group, with an inhibitory rate of approximately 80% (Fig. 5C). Compared with those in the vehicle group, TUNEL-positive cells were observed approximately 3-fold more clearly in the tumors in the digitoxin-treated groups (Fig. 5D). To further confirm whether digitoxin exerts its anticancer effects *in vivo* by activating the caspase pathway, the protein levels of cleaved caspase-3 were detected in tumor tissues. As was expected, cleaved caspase-3 was strongly increased (Fig. 5E and F). In addition, Ki-67 staining was used to examine the effects of digitoxin on tumor proliferation, and the results demonstrated that the number of Ki-67-positive cells were reduced by >50% in the digitoxin-treated groups compared with the control group (Fig. 5F). Of note, compared with the control group, digitoxin treatment did not lead to a reduction in body weight at the end of treatment (Fig. S1), and mice in the digitoxin group did not exhibit any abnormalities in food intake or behavior, suggesting that digitoxin may exhibit low or no toxicity at the doses used in the present study. Furthermore, pathological analysis of the heart demonstrated that there were no apparent changes in the digitoxin-treated tumor-bearing mice (Fig. 5G).

In summary, a library of 78 natural products was screened, and digitoxin exhibited the highest cytotoxicity against cervical cancer HeLa cells. Mechanistically, digitoxin caused DNA DSBs and then blocked the cell cycle at the G_2/M phase via the ATM/ATR-CHK1/CHK2-Cdc25C pathway. In addition, the accumulation of cytochrome *c* caused by the digitoxin-induced activation of caspase-9 and caspase-3, ultimately triggered the

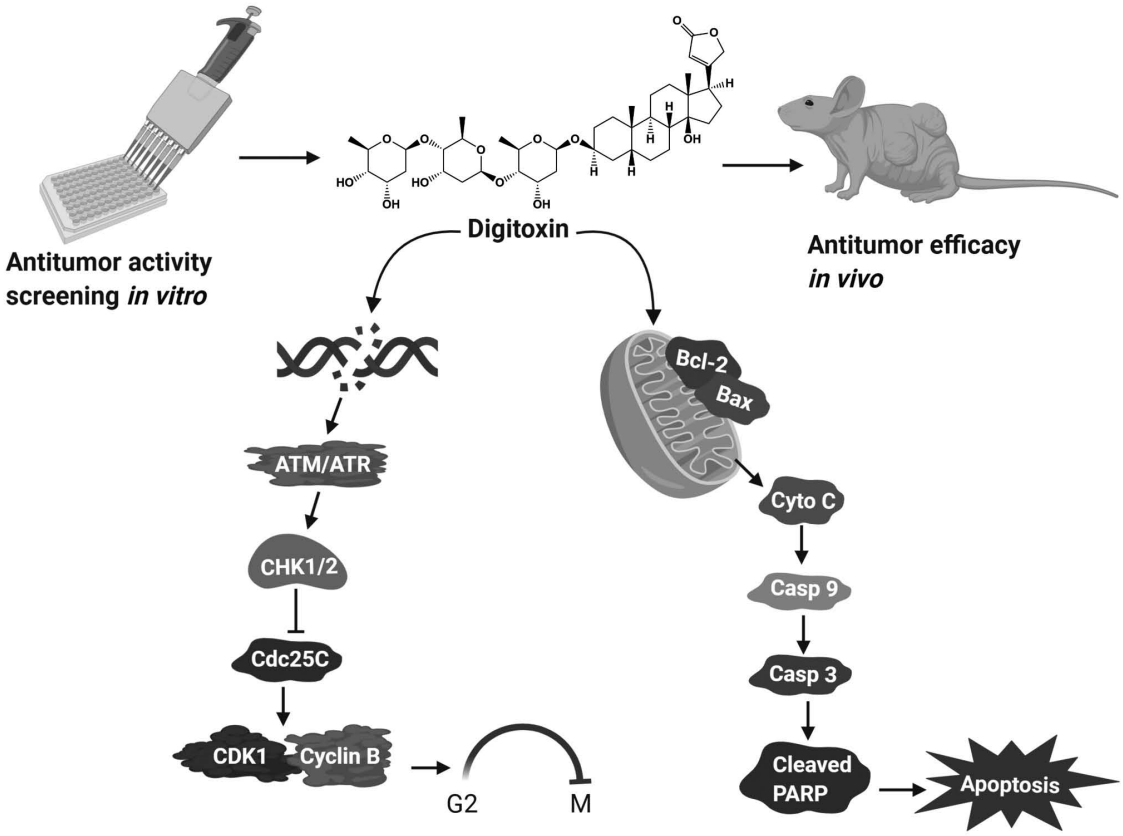

Figure 6. Digitoxin inhibited HeLa cell growth through G_2/M arrest and apoptosis. A library of 78 natural products was screened, and digitoxin exhibited the highest cytotoxicity against cervical cancer HeLa cells. Mechanistically, digitoxin caused DNA double-stranded breaks and then blocked the cell cycle at the G_2/M phase via the ATM/ATR-CHK1/CHK2-Cdc25C pathway. In addition, the accumulation of cytochrome c caused by the digitoxin-induced activation of caspase-9 and caspase-3, ultimately triggered mitochondrial apoptosis of HeLa cells. Moreover, the *in vivo* anticancer effects of digitoxin were confirmed in HeLa cell xenotransplantation models. These data indicate that digitoxin is an effective therapeutic agent for cervical cancer.

mitochondrial apoptosis of HeLa cells (Fig. 6). Moreover, the *in vivo* anticancer effects of digitoxin were confirmed in HeLa cell xenotransplantation models. These data indicate that digitoxin is an effective therapeutic agent for cervical cancer.

Discussion

Traditionally, natural products, such as colchicine, doxorubicin hydrochloride, vinblastine (VBL) and paclitaxel (Taxol®), have been one of the primary sources of drug discovery in the field of cancer research and are among the most effective cancer chemotherapeutics that are currently available (42-44). In previously published data, the IC_{50} values of colchicine and doxorubicin hydrochloride against HeLa cells were shown to be 1.08 and 0.374 μM (45,46), respectively. In the present study, digitoxin displayed potent antiproliferative activity with an IC_{50} value of 0.028 μM. According to these data, digitoxin appears to have at least as much antitumor activity as colchicine and doxorubicin hydrochloride against HeLa cells *in vitro*. Of note, Hosseini *et al* reported that digitoxin exerted cytotoxic effects against HeLa cells with an IC_{50} value of 5.62 μg/ml (47), which is different from the value observed in the present study. There may be several reasons for this difference, including the cell culture conditions, the experimental details of the cell viability assay, and the storage concentration of digitoxin.

In detail, it was found that digitoxin induced DSBs and then triggered the DNA damage response ATM/ATR-CHK1/CHK2-Cdc25C pathway in human cervical cancer HeLa cells. It has been reported that a number of small molecules can arrest the cell cycle at the G_1/S or S phase to prevent incorrect DNA replication or at the G_2/M phase to prevent entry into mitosis with damaged DNA (48). The present study found that digitoxin impeded cell cycle progression at the G_2/M phase, suggesting that digitoxin may not block DNA replication, but instead induce DNA damage. The DNA damage factors, phosphorylated ATM, ATR and γH2AX, accumulate upon the activation of DNA damage checkpoints (49,50), as observed in the present study. CHK2 is phosphorylated by ATM (39), and CHK1 is activated by the ATR-dependent phosphorylation (40). Activated CHK2 and CHK1 inactive Cdc25C to maintain the CDK1-Cyclin B1 complex in an inactivate state in the G_2 phase, thereby inhibiting the G_2/M transition (41). In the present study, the CHK1 and CHK2 kinases were activated, and the levels of the Cdc25C phosphatase were downregulated. Overall, these data demonstrated that digitoxin induced DNA damage and ultimately led to G_2/M cell cycle arrest via the ATM/ATR-CHK1/CHK2-Cdc25C pathway in HeLa cells.

It has been reported that digitoxin blocks the cell cycle at the G_2/M phase by decreasing the expression of both cyclin B1 and CDK1 in NCI-H460 and H1975 lung cancer cells (17,51). Accordingly, the present study also found that digitoxin significantly decreased the protein expression levels of total CDK1 and phosphorylated (p-CDK1 Thr14). However, digitoxin treatment led to a marked accumulation of cyclin B1 protein in

HeLa cells. This evidence indicates that the molecular mechanisms through which digitoxin modulates the cell cycle may be context-dependent. In eukaryotic cells, the expression of cyclin B1 is very low in the G_1 phase, is synthesized and significantly increased in the S phase, and peaks at the late G_2 phase and early mitosis. When cells enter late mitosis, the expression of cyclin B1 is significantly decreased (52-56). In the present study, the cell population in the G_2/M phase was increased in the presence of digitoxin, suggesting that digitoxin consistently triggered G_2/M phase arrest, and the accumulation of cyclin B1 protein in digitoxin-treated HeLa cells further suggested that digitoxin led to G_2/M arrest. Nevertheless, the reasons for this differential effect of digitoxin are complex and warrant further investigation in the future.

Digitoxin, as a Na^+/K^+-ATPase inhibitor, is widely applied in the clinical management of heart diseases, such as congestive heart failure and cardiac arrhythmias (57). It should be noted that digitoxin may cause cardiac side-effects. It has been demonstrated that digitoxin leads to poisoning at serum concentrations of 108-205 ng/ml (approximately 140-270 nM) (15,58). Other studies have reported that digitoxin exerts anticancer effects at concentrations ranging from 20 to 33 nM, and no notable toxicity has been observed in cardiac patients (16,59). As previously demonstrated, the growth of tumors was attenuated effectively in mice bearing M214 melanomas after 27 days digitoxin treatment and no cardiac side-effects were observed (60). In the present study, it was found that digitoxin exhibited cytotoxicity in HeLa cells with an IC_{50} value of approximately 28 nM and the mechanism involved was digitoxin-induced G_2/M phase cell cycle arrest at concentrations of 4 and 20 nM. *In vivo*, compared with the control treatment, digitoxin treatment did not lead to a reduction in body weight at the end of treatment, and mice in the digitoxin group did not exhibit any abnormalities in food intake or behavior, and heart pathological analysis demonstrated that there were no apparent changes in digitoxin-treated tumor-bearing mice. Combining the results from others laboratories with the current experimental data, it is suggested that digitoxin does not cause cardiac side-effects at the concentration used in the present study. Furthermore, digitoxin has been demonstrated to exert a notable killing effect on HeLa cells (IC_{50} = 5.62 μg/ml), but to cause almost no damage to normal human lymphocyte cells (IC_{50} = 412.94 μg/ml) (47). Previous studies have proven that the cardiac glycosides are generally more toxic to cancer cells than normal peripheral blood mononuclear cells (34,61,62). Thus, digitoxin has few adverse side-effects on normal human cells at the concentration used in the present study. However, prospective clinical trials need to be performed to determine whether digitoxin is useful as an anticancer agent.

Several trials related to the use of digitoxin in combination with other anticancer agents are currently reported. For example, the combination of digitoxin with standard chemotherapeutic agents in clinical practice, such as 5-fluorouracil, cisplatin and oxaliplatin, has additive effects against colon cancer HT-29 and HCT116 cells (63). Digitoxin and its synthetic analog, MonoD, exert potent anti-proliferative effects at clinically relevant concentrations in serum-starved conditions, while paclitaxel, hydroxyurea and colchicine were only active in lung cancer cells growing in routine culture conditions. Furthermore, digitoxin and its analog have been shown to potentiate the effects of hydroxyurea or paclitaxel (64). These data indicate that digitoxin has potential clinical applications in translational oncology particularly in combination with other drugs.

In conclusion, the present study screened a library of natural compounds composed of 78 single compounds to identify potential lead compounds with activity against cervical cancer, and digitoxin exhibited the highest cytotoxicity in the different malignant cell lines. Mechanistically, digitoxin causes DNA DSBs, blocks the cell cycle at the G_2/M phase via the ATM/ATR-CHK1/CHK2-Cdc25C pathway, and ultimately triggers mitochondrial apoptosis. Furthermore, the *in vivo* anticancer effects of digitoxin were confirmed in HeLa cell xenotransplantation models. These results shed new light on the mechanisms of digitoxin-induced cell cycle arrest, which is valuable for the further study of the application of digitoxin to anticancer chemotherapy in clinical practice.

Acknowledgements

Not applicable.

Funding

The present study was supported by the National Science Foundation of China (grant nos. 81803790, 81630104 and 81973748), the National Natural Science Foundation of Guangdong (grant no. 2020A1515011090) and the Huang Zhendong Research Fund for Traditional Chinese Medicine of Jinan University.

Availability of data and materials

All data generated or analyzed during this study are included in this published article or are available from the corresponding author upon reasonable request.

Authors' contributions

LD and JC designed the study and revised the manuscript. HG, MQ and CC performed the experiments and drafted the manuscript. PL, YL and GY assisted with the *in vitro* research experiments. AL and FX contributed to the flow cytometry experiments. WY and DZ assisted with the design of the study and revised the manuscript. DL assisted with the revision of the manuscript and performed experiments to update the data. All authors have read and approved the final manuscript.

Ethics approval and consent to participate

All animal experiments were conducted in compliance with the ARRIVE guidelines and were approved by the Experimental Animal Ethics Committee of Jinan University (Guangzhou, China).

Patient consent for publication

Not applicable.

Competing interests

The authors declare that they have no competing interests.

References

1. Bonde JH, Sandri MT, Gary DS and Andrews JC: Clinical utility of human papillomavirus genotyping in cervical cancer screening: A systematic review. J Low Genit Tract Dis 24: 1-13, 2020.
2. Wang R, Pan W, Jin L, Huang W, Li Y, Wu D, Gao C, Ma D and Liao S: Human papillomavirus vaccine against cervical cancer: Opportunity and challenge. Cancer Lett 471: 88-102, 2020.
3. Eskander RN and Tewari KS: Chemotherapy in the treatment of metastatic, persistent, and recurrent cervical cancer. Curr Opin Obstet Gynecol 26: 314-321, 2014.
4. Monk BJ and Tewari KS: Evidence-based therapy for recurrent cervical cancer. J Clin Oncol 32: 2687-2690, 2014.
5. Liontos M, Kyriazoglou A, Dimitriadis I, Dimopoulos MA and Bamias A: Systemic therapy in cervical cancer: 30 years in review. Crit Rev Oncol Hematol 137: 9-17, 2019.
6. Li H, Wu X and Cheng X: Advances in diagnosis and treatment of metastatic cervical cancer. J Gynecol Oncol 27: e43, 2016.
7. Gokduman K: Strategies targeting DNA topoisomerase I in cancer chemotherapy: Camptothecins, nanocarriers for camptothecins, organic non-camptothecin compounds and metal complexes. Curr Drug Targets 17: 1928-1939, 2016.
8. Khanna C, Rosenberg M and Vail DM: A review of paclitaxel and novel formulations including those suitable for use in dogs. J Vet Intern Med 29: 1006-1012, 2015.
9. Newman DJ and Cragg GM: Natural products as sources of new drugs over the 30 years from 1981 to 2010. J Nat Prod 75: 311-335, 2012.
10. Carter GT: Natural products and Pharma 2011: Strategic changes spur new opportunities. Nat Prod Rep 28: 1783-1789, 2011.
11. Cragg GM and Newman DJ: Natural products: A continuing source of novel drug leads. Biochim Biophys Acta 1830: 3670-3695, 2013.
12. Harvey AL, Edrada-Ebel R and Quinn RJ: The re-emergence of natural products for drug discovery in the genomics era. Nat Rev Drug Discov 14: 111-129, 2015.
13. Mishra BB and Tiwari VK: Natural products: An evolving role in future drug discovery. Eur J Med Chem 46: 4769-4807, 2011.
14. Newman DJ and Cragg GM: Natural products as sources of new drugs from 1981 to 2014. J Nat Prod 79: 629-661, 2016.
15. Patel S: Plant-derived cardiac glycosides: Role in heart ailments and cancer management. Biomed Pharmacother 84: 1036-1041, 2016.
16. López-Lázaro M, Pastor N, Azrak SS, Ayuso MJ, Austin CA and Cortés F: Digitoxin inhibits the growth of cancer cell lines at concentrations commonly found in cardiac patients. J Nat Prod 68: 1642-1645, 2005.
17. Zhang YZ, Chen X, Fan XX, He JX, Huang J, Xiao DK, Zhou YL, Zheng SY, Xu JH, Yao XJ, *et al*: Compound library screening identified cardiac glycoside digitoxin as an effective growth inhibitor of gefitinib-resistant non-small cell lung cancer via downregulation of α-tubulin and inhibition of microtubule formation. Molecules 21: 374, 2016.
18. Iyer AKV, Zhou M, Azad N, Elbaz H, Wang L, Rogalsky DK, Rojanasakul Y, O'Doherty GA and Langenhan JM: A direct comparison of the anticancer activities of digitoxin MeON-Neoglycosides and O-Glycosides: Oligosaccharide chain length-dependent induction of caspase-9-mediated apoptosis. ACS Med Chem Lett 1: 326-330, 2010.
19. Trenti A, Boscaro C, Tedesco S, Cignarella A, Trevisi L and Bolego C: Effects of digitoxin on cell migration in ovarian cancer inflammatory microenvironment. Biochem Pharmacol 154: 414-423, 2018.
20. Hsu IL, Chou CY, Wu YY, Wu JE, Liang CH, Tsai YT, Ke JY, Chen YL, Hsu KF and Hong TM: Targeting FXYD2 by cardiac glycosides potently blocks tumor growth in ovarian clear cell carcinoma. Oncotarget 7: 62925-62938, 2016.
21. Prassas I, Karagiannis GS, Batruch I, Dimitromanolakis A, Datti A and Diamandis EP: Digitoxin-induced cytotoxicity in cancer cells is mediated through distinct kinase and interferon signaling networks. Mol Cancer Ther 10: 2083-2093, 2011.
22. Shang Z and Zhang L: Digitoxin increases sensitivity of glioma stem cells to TRAIL-mediated apoptosis. Neurosci Lett 653: 19-24, 2017.
23. Lee DH, Cheul Oh S, Giles AJ, Jung J, Gilbert MR and Park DM: Cardiac glycosides suppress the maintenance of stemness and malignancy via inhibiting HIF-1α in human glioma stem cells. Oncotarget 8: 40233-40245, 2017.
24. Pollard BS, Suckow MA, Wolter WR, Starr JM, Eidelman O, Dalgard CL, Kumar P, Battacharyya S, Srivastava M, Biswas R, *et al*: Digitoxin Inhibits epithelial-to-mesenchymal-transition in hereditary castration resistant prostate cancer. Front Oncol 9: 630, 2019.
25. Liu M, Feng LX, Sun P, Liu W, Mi T, Lei M, Wu W, Jiang B, Yang M, Hu L, *et al*: Knockdown of apolipoprotein E enhanced sensitivity of Hep3B cells to cardiac steroids via regulating Na^+/K^+-ATPase signalosome. Mol Cancer Ther 15: 2955-2965, 2016.
26. Felth J, Rickardson L, Rosén J, Wickström M, Fryknäs M, Lindskog M, Bohlin L and Gullbo J: Cytotoxic effects of cardiac glycosides in colon cancer cells, alone and in combination with standard chemotherapeutic drugs. J Nat Prod 72: 1969-1974, 2009.
27. Xiao Y, Yan W, Guo L, Meng C, Li B, Neves H, Chen PC, Li L, Huang Y, Kwok HF, *et al*: Digitoxin synergizes with sorafenib to inhibit hepatocelluar carcinoma cell growth without inhibiting cell migration. Mol Med Rep 15: 941-947, 2017.
28. Einbond LS, Shimizu M, Ma H, Wu HA, Goldsberry S, Sicular S, Panjikaran M, Genovese G and Cruz E: Actein inhibits the Na+-K+-ATPase and enhances the growth inhibitory effect of digitoxin on human breast cancer cells. Biochem Biophys Res Commun 375: 608-613, 2008.
29. Einbond LS, Wu HA, Sandu C, Ford M, Mighty J, Antonetti V, Redenti S and Ma H: Digitoxin enhances the growth inhibitory effects of thapsigargin and simvastatin on ER negative human breast cancer cells. Fitoterapia 109: 146-154, 2016.
30. Kulkarni YM, Kaushik V, Azad N, Wright C, Rojanasakul Y, O'Doherty G and Iyer AK: Autophagy-induced apoptosis in lung cancer cells by a novel digitoxin analog. J Cell Physiol 231: 817-828, 2016.
31. Trenti A, Zulato E, Pasqualini L, Indraccolo S, Bolego C and Trevisi L: Therapeutic concentrations of digitoxin inhibit endothelial focal adhesion kinase and angiogenesis induced by different growth factors. Br J Pharmacol 174: 3094-3106, 2017.
32. Deng LJ, Peng QL, Wang LH, Xu J, Liu JS, Li YJ, Zhuo ZJ, Bai LL, Hu LP, Chen WM, *et al*: Arenobufagin intercalates with DNA leading to G2 cell cycle arrest via ATM/ATR pathway. Oncotarget 6: 34258-34275, 2015.
33. Silva IT, Munkert J, Nolte E, Zanchett Schneider NF, Carvalho Rocha S, Pacheco Ramos AC, Kreis W, Castro Braga F, de Pádua RM, *et al*: Cytotoxicity of AMANTADIG - a semi-synthetic digitoxigenin derivative - alone and in combination with docetaxel in human hormone-refractory prostate cancer cells and its effect on Na^+/K^+-ATPase inhibition. Biomed Pharmacother 107: 464-474, 2018.
34. Johansson S, Lindholm P, Gullbo J, Larsson R, Bohlin L and Claeson P: Cytotoxicity of digitoxin and related cardiac glycosides in human tumor cells. Anticancer Drugs 12: 475-483, 2001.
35. Marzo-Mas A, Barbier P, Breuzard G, Allegro D, Falomir E, Murga J, Carda M, Peyrot V and Marco JA: Interactions of long-chain homologues of colchicine with tubulin. Eur J Med Chem 126: 526-535, 2017.
36. Stark GR and Taylor WR: Control of the G2/M transition. Mol Biotechnol 32: 227-248, 2006.
37. Kastan MB and Bartek J: Cell-cycle checkpoints and cancer. Nature 432: 316-323, 2004.
38. Löbrich M, Shibata A, Beucher A, Fisher A, Ensminger M, Goodarzi AA, Barton O and Jeggo PA: gammaH2AX foci analysis for monitoring DNA double-strand break repair: Strengths, limitations and optimization. Cell Cycle 9: 662-669, 2010.
39. Matsuoka S, Rotman G, Ogawa A, Shiloh Y, Tamai K and Elledge SJ: Ataxia telangiectasia-mutated phosphorylates Chk2 in vivo and in vitro. Proc Natl Acad Sci USA 97: 10389-10394, 2000.
40. Zhao H and Piwnica-Worms H: ATR-mediated checkpoint pathways regulate phosphorylation and activation of human Chk1. Mol Cell Biol 21: 4129-4139, 2001.
41. Perdiguero E and Nebreda AR: Regulation of Cdc25C activity during the meiotic G2/M transition. Cell Cycle 3: 733-737, 2004.
42. Gupta S and Bhattacharyya B: Antimicrotubular drugs binding to vinca domain of tubulin. Mol Cell Biochem 253: 41-47, 2003.
43. Jordan MA, Thrower D, Wilson L, Jordan MA, Thrower D and Wilson L: Mechanism of inhibition of cell proliferation by Vinca alkaloids. Cancer Res 51: 2212-2222, 1991.
44. Johnson IS, Armstrong JG, Gorman M and Burnett JP Jr: The vinca alkaloids, a new class of oncolytic agents. Cancer Res 23: 1390-1427, 1963.
45. Sadeghi-Aliabadi H, Minaiyan M and Dabestan A: Cytotoxic evaluation of doxorubicin in combination with simvastatin against human cancer cells. Res Pharm Sci 5: 127-133, 2010.
46. Yin Y, Lian BP, Xia YZ, Shao YY and Kong LY: Design, synthesis and biological evaluation of resveratrol-cinnamoyl derivates as tubulin polymerization inhibitors targeting the colchicine binding site. Bioorg Chem 93: 103319, 2019.

47. Hosseini M, Taherkhani M and Ghorbani Nohooji M: Introduction of Adonis aestivalis as a new source of effective cytotoxic cardiac glycoside. Nat Prod Res 33: 915-920, 2019.
48. Laiho M and Latonen L: Cell cycle control, DNA damage checkpoints and cancer. Ann Med 35: 391-397, 2003.
49. Harper JW and Elledge SJ: The DNA damage response: Ten years after. Mol Cell 28: 739-745, 2007.
50. Durocher D and Jackson SP: DNA-PK, ATM and ATR as sensors of DNA damage: variations on a theme? Curr Opin Cell Biol 13: 225-231, 2001.
51. Elbaz HA, Stueckle TA, Wang HYL, O'Doherty GA, Lowry DT, Sargent LM, Wang L, Dinu CZ and Rojanasakul Y: Digitoxin and a synthetic monosaccharide analog inhibit cell viability in lung cancer cells. Toxicol Appl Pharmacol 258: 51-60, 2012.
52. Nurse P: A long twentieth century of the cell cycle and beyond. Cell 100: 71-78, 2000.
53. Bloom J and Cross FR: Multiple levels of cyclin specificity in cell-cycle control. Nat Rev Mol Cell Biol 8: 149-160, 2007.
54. Fisher DL and Nurse P: A single fission yeast mitotic cyclin B p34cdc2 kinase promotes both S-phase and mitosis in the absence of G1 cyclins. EMBO J 15: 850-860, 1996.
55. Hayles J, Fisher D, Woollard A and Nurse P: Temporal order of S phase and mitosis in fission yeast is determined by the state of the p34cdc2-mitotic B cyclin complex. Cell 78: 813-822, 1994.
56. Gould KL and Nurse P: Tyrosine phosphorylation of the fission yeast cdc2+ protein kinase regulates entry into mitosis. Nature 342: 39-45, 1989.
57. Rahimtoola SH: Digitalis therapy for patients in clinical heart failure. Circulation 109: 2942-2946, 2004.
58. Lapostolle F, Borron SW, Verdier C, Taboulet P, Guerrier G, Adnet F, Clemessy JL, Bismuth C and Baud FJ: Digoxin-specific Fab fragments as single first-line therapy in digitalis poisoning. Crit Care Med 36: 3014-3018, 2008.
59. Haux J, Klepp O, Spigset O and Tretli S: Digitoxin medication and cancer; case control and internal dose-response studies. BMC Cancer 1: 11, 2001.
60. Eskiocak U, Ramesh V, Gill JG, Zhao Z, Yuan SW, Wang M, Vandergriff T, Shackleton M, Quintana E, Johnson TM, *et al*: Synergistic effects of ion transporter and MAP kinase pathway inhibitors in melanoma. Nat Commun 7: 12336, 2016.
61. Daniel D, Süsal C, Kopp B, Opelz G and Terness P: Apoptosis-mediated selective killing of malignant cells by cardiac steroids: maintenance of cytotoxicity and loss of cardiac activity of chemically modified derivatives. Int Immunopharmacol 3: 1791-1801, 2003.
62. López-Lázaro M: Digitoxin as an anticancer agent with selectivity for cancer cells: Possible mechanisms involved. Expert Opin Ther Targets 11: 1043-1053, 2007.
63. Zhao B, Kim J, Ye X, Lai ZC and Guan KL: Both TEAD-binding and WW domains are required for the growth stimulation and oncogenic transformation activity of yes-associated protein. Cancer Res 69: 1089-1098, 2009.
64. Yakisich JS, Azad N, Venkatadri R, Kulkarni Y, Wright C, Kaushik V, O'Doherty GA and Iyer AK: Digitoxin and its synthetic analog MonoD have potent antiproliferative effects on lung cancer cells and potentiate the effects of hydroxyurea and paclitaxel. Oncol Rep 35: 878-886, 2016.